Published by
NIGERIAN SOCIETY OF PHYSICAL SCIENCES
Available online @ https://asr.nsps.org.ng/index.php/asr

African Scientific Reports 5 (2026) 546

African Scientific Reports

Integrated geophysical, geochemical and remote sensing assessment of soil corrosion susceptibility in Sabon Gida, Katsina State, Northwestern Nigeria

Akpaneno A. Francis[a,*], Ahmad Abdulhakim[a,b]

[a]Department of Geophysics, Federal University Dutsin-Ma, P.M.B 5001. Dutsin-Ma, Katsina State, Nigeria
[b]Department of Physics, School of General Studies, Federal University of Transportation Daura, P.M.B. 1050, Daura, Katsina State, Nigeria

Abstract

One of the major factors affecting the longevity of buried metallic infrastructure, including pipelines, underground tanks, and foundation materials, is soil corrosivity. This study integrated geophysical, geochemical, and remote sensing data to assess soil corrosion susceptibility in Sabon Gida, Katsina State, Nigeria. The Schlumberger array configuration was used to acquire vertical electrical sounding (VES) data at 44 stations to evaluate subsurface resistivity and corrosion potential. Soil samples were collected at depths of 0–0.5, 0.5–1.0, 1.0–1.5, and 1.5–2.0 m from five representative VES locations corresponding to different resistivity classes and analyzed for pH. Sentinel-2 Level-2A imagery was processed to derive the normalized difference vegetation index (NDVI), normalized difference water index (NDWI), bare soil index (BSI), and salinity index (SI). The analytical hierarchy process (AHP) and weighted sum model (WSM) were integrated within a geographic information system (GIS) to generate a corrosion susceptibility index (CSI) map. The interpreted resistivity values ranged from 23.11 to 1779 Ω m, indicating significant spatial variation in subsurface conductivity. Soil pH values ranged from 6.3 to 7.1, reflecting slightly acidic to near-neutral conditions. The remote sensing indices revealed spatial variations in vegetation cover, moisture conditions, salinity, and bare soil exposure across the study area. The resulting CSI map indicates predominantly moderate corrosion susceptibility across the study area on 2 to 3 scale of corrosion susceptibility level suggesting relatively favorable conditions for buried infrastructure. However, site-specific engineering investigations and direct corrosion measurements are recommended before installation. The integrated approach provides a more comprehensive assessment than single-parameter methods and offers valuable information for infrastructure planning and corrosion management in the study area.

DOI: 10.46481/asr.2026.5.2.546

Keywords: Soil corrosivity, Electrical resistivity, Analytical hierarchy process, Corrosion susceptibility, Remote sensing

Article history:
Received: 15 May 2026
Received in revised form: 18 June 2026
Accepted for publication: 23 June 2026
Available online: 30 July 2026

1. Introduction

One of the major engineering and environmental challenges affecting pipelines, subterranean storage systems, and other subsurface infrastructure is corrosion of buried metallic components. Several soil properties, including salinity, moisture content, pH, and

*Corresponding author Tel. No.: +234-803-503-7159.
Email address: aakpaneno@fudutsinma.edu.ng (Akpaneno A. Francis)

clay content, influence soil conductivity and corrosion processes. These factors regulate electrochemical reactions that can accelerate the deterioration of buried metallic structures [1, 2].

Because electrical resistivity represents the combined effects of dissolved ions, moisture content, and soil texture, it is widely recognized as one of the most reliable indicators of soil corrosivity [3]. Low resistivity values are typically associated with high conductivity, moisture retention, and high ionic concentration, which are conditions that can increase corrosion processes.

Electrical resistivity studies and geochemical soil evaluations are commonly used in conventional corrosion assessment methods. Although these methods provide reliable data at specific points, they are usually limited in capturing spatial variability across broad areas [4]. Recent advances in remote sensing and geographic information system (GIS) approaches have improved environmental monitoring by enabling spatial assessment of surface characteristics related to soil properties and moisture conditions [5, 6].

Sentinel-2 multispectral imagery provides high- to medium-resolution data appropriate for land-surface and environmental studies. Spectral indices derived from Sentinel-2 data have been used successfully to assess soil and environmental conditions, including surface moisture, water, salinity, and vegetation conditions [5, 6]. Subsurface conductivity is influenced by factors such as salinity, moisture, and vegetation cover, which can also affect corrosion susceptibility.

Previous studies in Nigeria on soil corrosion susceptibility have primarily focused on geoelectrical measurements or physicochemical soil properties as standalone indicators of corrosion risk. Although these approaches provide valuable information, they may not adequately capture the spatial variability of environmental factors that influence corrosion processes. Recent advances in remote sensing and GIS technologies offer opportunities for integrating subsurface and surface environmental datasets for improved corrosion assessment. However, studies that combine geophysical measurements, geochemical indicators, Sentinel-2 remote sensing indices, GIS, and multi-criteria decision analysis for corrosion susceptibility mapping remain scarce in semi-arid regions of Northwestern Nigeria. This study addresses this gap by integrating electrical resistivity, soil pH, vegetation, moisture, salinity, and bare-soil indicators within an analytical hierarchy process (AHP)-based GIS framework to develop a spatial corrosion susceptibility model for Sabon Gida, Katsina State.

2. Study area

The study area, Sabon Gida, is located along Jibia Road in Katsina State, at approximately latitude 13°00′35.01″ N and longitude 7°34′29.26″ E (Figure 1). Sabon Gida, and Katsina State more generally, is part of the Sudan Savanna ecological zone, with clearly defined wet and dry seasons [7, 8]. Katsina experiences temperatures of about 30–42 °C, with annual rainfall of 600–800 mm received within 2–3 months of the year. Vegetation in the area is generally moderate, especially in Sabon Gida, while some parts of Katsina remain relatively dry because of the semi-arid climatic conditions [8]. Geologically, the study area is part of the Nigerian Basement Complex, which is predominantly composed of gneissic and granitic rocks [9–12].

The need for environmental evaluation and preservation of subsurface engineering assets in the region has increased as a result of rapid urban expansion, including the construction of gas plants, fuel stations, and commercial buildings.

3. Materials and methods

3.1. Electrical resistivity survey

The vertical electrical sounding (VES) method with the Schlumberger electrode configuration was used in this study to obtain electrical resistivity measurements [3, 13]. A total of 44 VES stations with current electrode spacing ($AB/2$) ranging from 2 to 30 m and potential electrode spacing ($MN/2$) kept constant at 1 m were located within the study area. Measurements were acquired using a Herojat Rhomega electrical resistivity meter.

In this study, the apparent resistivity (ρ_a) was calculated using Eq. (1):

$$\rho_a = K \times R, \tag{1}$$

where the geometric factor K for the Schlumberger array was calculated using Eq. (2):

$$K = \frac{\pi\left(AB^2 - MN^2\right)}{4MN}. \tag{2}$$

In Eqs. (1) and (2), AB is the distance between the two current electrodes, MN is the distance between the two potential electrodes, ρ_a is the apparent resistivity (Ω m), K is the geometric factor, and R is the measured resistance (Ω).

The calculated apparent resistivity values were interpreted using IPI2Win software to obtain layer resistivities, thicknesses, and depths [14]. Resistivity values corresponding to depths less than or equal to 2 m were extracted because such depths commonly correspond to the burial levels of underground engineering infrastructure [15–17]. Soil corrosion was classified based on standard soil resistivity ranges recommended by ASTM International and NACE International, as summarized in Table 1 [15–17].

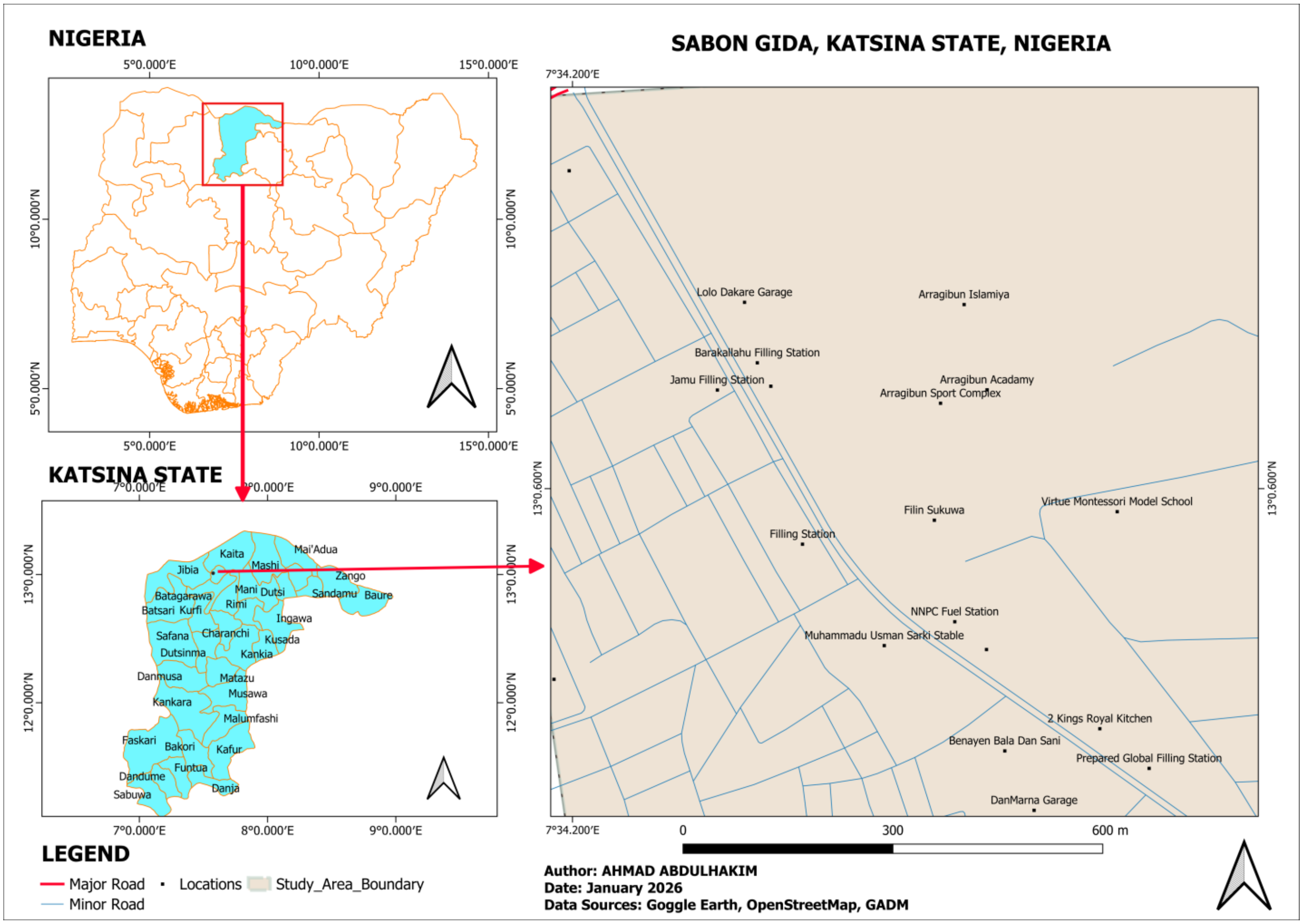

Figure 1: Location map of the study area.

Table 1: Combined ASTM and NACE soil corrosivity classification based on soil resistivity.

Soil resistivity (Ω m)	ASTM G57 classification	NACE classification	Adopted corrosion risk level
< 100	Very highly corrosive	Severe	Very highly corrosive
100–300	Highly corrosive	High	Highly corrosive
300–500	Highly corrosive	Moderate–high	Moderate–high
500–1000	Moderately corrosive	Moderate	Moderate
> 1000	Slightly corrosive	Low	Slightly/low

3.2. Soil pH analysis

Five representative VES locations were selected for soil sampling to ensure coverage of the full range of resistivity conditions identified across the study area, namely very highly corrosive, highly corrosive, moderate-high corrosive, moderate corrosive, and slightly corrosive zones. Soil samples were collected at depth intervals of 0–0.5, 0.5–1.0, 1.0–1.5, and 1.5–2.0 m using a hand auger, yielding a total of 20 samples. The sampling strategy provided representative information on soil acidity conditions while considering field accessibility and laboratory analysis constraints. Soil pH classification and associated corrosion susceptibility were adopted from standard soil science and corrosion classification schemes, as shown in Table 2 [18, 19].

3.3. Remote sensing data processing

The study used Sentinel-2 Level-2A imagery obtained in February and March 2026, corresponding to the period of field investigation. The imagery was downloaded from the Copernicus Open Access Hub, the official data distribution platform of the European Space Agency (ESA). The QGIS environment was used to process the imagery, which was acquired in atmospherically corrected Level-2A surface reflectance form.

Table 2: Soil pH classification.

Soil pH	Soil condition	Corrosion susceptibility
< 5.5	Strongly acidic	Very high
5.5–6.5	Moderately acidic	High
6.5–7.5	Near neutral	Neutral
> 7.5	Alkaline	Low

Source: Adapted from Refs. [18, 19].

Table 3: AHP pairwise comparison scale.

Scale	Interpretation
1	Equal importance
3	Moderate importance
5	Strong importance
7	Very strong importance
9	Extreme importance
2, 4, 6, 8	Intermediate values

Source: Ref. [20].

Image preprocessing involved layer stacking of spectral bands, subsetting the images to the study area, and confirming spatial alignment. Four spectral indices related to environmental factors that can affect soil corrosion were generated. The normalized difference vegetation index (NDVI) was computed using the near-infrared (NIR; B08) and red (B04) bands, as shown in Eq. (3) [21–23]:

$$\mathrm{NDVI} = \frac{\mathrm{NIR} - \mathrm{Red}}{\mathrm{NIR} + \mathrm{Red}}. \tag{3}$$

The normalized difference water index (NDWI) was computed using the green (B03) and NIR (B08) bands, as shown in Eq. (4) [24]:

$$\mathrm{NDWI} = \frac{\mathrm{Green} - \mathrm{NIR}}{\mathrm{Green} + \mathrm{NIR}}. \tag{4}$$

The bare soil index (BSI) was computed using the short-wave infrared (SWIR; B11), red (B04), NIR (B08), and blue (B02) bands, as shown in Eq. (5) [25, 26]:

$$\mathrm{BSI} = \frac{(\mathrm{Red} + \mathrm{SWIR}) - (\mathrm{NIR} + \mathrm{Blue})}{(\mathrm{Red} + \mathrm{SWIR}) + (\mathrm{NIR} + \mathrm{Blue})}. \tag{5}$$

The salinity index (SI) was computed using the SWIR (B11) and red (B04) bands, as shown in Eq. (6) [27]:

$$\mathrm{SI} = \frac{\mathrm{SWIR} - \mathrm{Red}}{\mathrm{SWIR} + \mathrm{Red}}. \tag{6}$$

The study-area vegetation characteristics, surface wetness, soil exposure, and salinity distribution were assessed using the derived indices in Eqs. (3)–(6).

3.4. Multi-criteria decision analysis

The governing factors were weighted using Saaty's AHP [20]. The Saaty comparison scale was used to compare the parameters pairwise (Table 3).

The relative importance of the six criteria considered in this study (electrical resistivity, soil pH, NDVI, NDWI, BSI, and SI) was established using literature evidence and expert judgment regarding their influence on soil corrosion processes [19, 20, 28]. Based on these priorities, a pairwise comparison matrix was constructed following the Saaty AHP framework to derive and validate the criterion weights used in the corrosion susceptibility model. The resulting matrix is presented in Table 4.

The pairwise comparison matrix shown in Table 4 was constructed following the AHP proposed by Saaty [20]. The relative importance assigned to each criterion reflects its perceived contribution to soil corrosion susceptibility based on literature evidence and expert judgment. Electrical resistivity was considered the most influential parameter because it directly reflects soil conductivity and corrosive potential [16, 19], followed by soil pH, vegetation conditions, moisture availability, bare-soil exposure, and salinity indicators.

The consistency of the pairwise comparison matrix was evaluated using the consistency index (CI) and consistency ratio (CR) proposed by Saaty [20]. The CI was calculated using Eq. (7):

$$\mathrm{CI} = \frac{\lambda_{\max} - n}{n - 1}, \tag{7}$$

Table 4: Reconstructed pairwise comparison matrix used for AHP weighting.

Criteria	Resistivity	pH	NDVI	NDWI	BSI	SI
Resistivity	1	2	3	4	4	7
pH	1/2	1	2	3	3	5
NDVI	1/3	1/2	1	2	2	3
NDWI	1/4	1/3	1/2	1	1	2
BSI	1/4	1/3	1/2	1	1	2
SI	1/7	1/5	1/3	1/2	1/2	1

Table 5: Consistency analysis of the AHP pairwise comparison matrix.

Parameter	Value
Number of criteria (n)	6
Maximum eigenvalue ($\lambda_{\max}$)	6.039
Consistency index (CI)	0.0078
Random index (RI)	1.24
Consistency ratio (CR)	0.0063
Consistency status	Acceptable (CR < 0.10)

where $\lambda_{\max}$ is the principal eigenvalue of the pairwise comparison matrix and n is the number of criteria. The CR was calculated using Eq. (8):

$$\mathrm{CR} = \frac{\mathrm{CI}}{\mathrm{RI}}, \tag{8}$$

where RI is the random index corresponding to the matrix size. A consistency ratio less than 0.10 indicates acceptable consistency in the pairwise comparison judgments [20]. The calculated CR value for this study was within the acceptable threshold, confirming the reliability of the assigned weights (Table 5).

Using the pairwise comparison matrix presented in Table 4, the maximum eigenvalue ($\lambda_{\max}$) was obtained as 6.039. The CI and CR were subsequently computed from Eqs. (7) and (8) as follows:

$$\mathrm{CI} = \frac{6.039 - 6}{6 - 1} = 0.0078,$$

and, for $n = 6$ and RI = 1.24,

$$\mathrm{CR} = \frac{0.0078}{1.24} = 0.0063.$$

The calculated CR value of 0.0063 is significantly lower than the acceptable threshold of 0.10, indicating a high level of consistency in the pairwise comparison judgments and confirming the reliability of the derived criterion weights [20].

The corrosion susceptibility index (CSI) was computed using the weighted sum model (WSM) [28], as shown in Eq. (9):

$$\mathrm{CSI} = \sum_{i=1}^{n} W_i S_i, \tag{9}$$

where W_i represents the assigned weight of each parameter and S_i represents the reclassified parameter score. The resulting CSI values were classified into corrosion susceptibility categories and mapped within the GIS environment [28].

The inverse distance weighting (IDW) interpolation technique in QGIS was used to generate continuous spatial surfaces for the corrosion susceptibility assessment. IDW was selected because of the relatively limited number of sampling locations and its ability to preserve local spatial variability under sparse data conditions. Previous geospatial and environmental studies have shown that IDW can provide useful interpolation results when data density is insufficient for robust geostatistical modeling [29].

Previous studies have shown that soil resistivity and soil pH are among the most important factors controlling soil corrosivity [19, 30, 31]. The weighting scheme adopted in this study was based on the relative influence of each parameter on corrosion processes reported in the literature. Electrical resistivity was assigned the highest weight (0.35) because it directly reflects soil conductivity, moisture retention, and ionic concentration, which are primary controls on corrosion development [16, 19, 30]. Soil pH was assigned a weight of 0.25 because of its influence on electrochemical reactions and metal dissolution [19, 31]. NDVI (0.15) and NDWI (0.10) were included to represent vegetation and moisture conditions that indirectly influence soil corrosivity through their effects on soil moisture retention and environmental conditions [5, 6, 23]. BSI was assigned a weight of 0.10 because exposed soil surfaces affect moisture dynamics and surface environmental conditions [21, 26]. SI was assigned a weight of 0.05 to account for the contribution of dissolved salts to soil conductivity and corrosion susceptibility [27, 31].

Table 6: Reclassification scheme for standardized remote sensing indices.

Index value	Interpretation	Score
> 0.6	Very high vegetation/moisture/salinity	5
0.4–0.6	High	4
0.2–0.4	Moderate	3
0.0–0.2	Low	2
< 0.0	Very low	1

Source: Modified after Ref. [21].

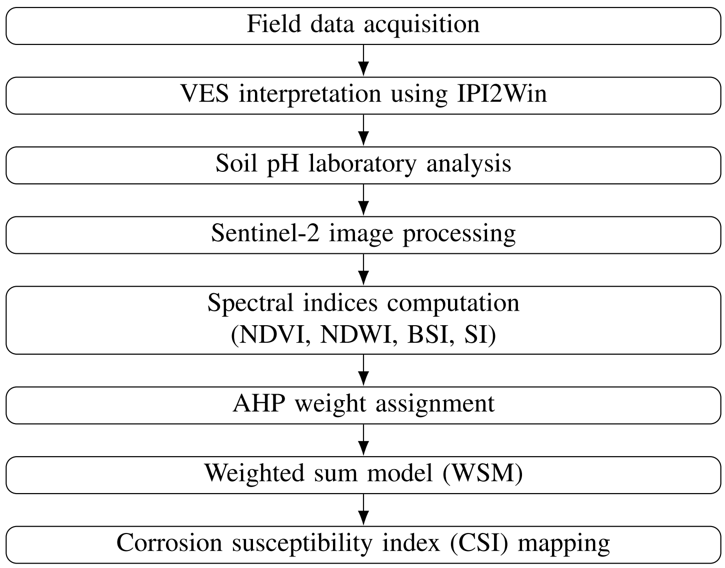

Figure 2: Methodological workflow adopted for corrosion susceptibility mapping.

For integration into the corrosion susceptibility model, the derived Sentinel-2 spectral indices were processed into standardized susceptibility scores. Based on the index value ranges in Table 6, the classification scheme used a five-class system ranging from very low to very high susceptibility [21].

4. Results

4.1. Electrical resistivity distribution

The interpreted apparent resistivity values obtained after inversion with IPI2Win for the 44 VES stations across the study area ranged from 23.11 to 1779 Ω m, showing variations in subsurface conditions. Locations such as VES 4, 5, 6, 38, and 39 showed very low resistivity values (below 100 Ω m) at shallow depths, suggesting zones of very high corrosion risk. These conductive zones are interpreted as areas with higher ionic concentration and moisture retention, which provide favorable conditions for corrosion processes [30, 31].

Moderately low resistivity values (100–300 Ω m) were observed at VES 7, 8, 9, 10, 11, 12, 13, and 17–18, among other stations. Higher resistivity values were observed at VES 14, 32, and 40 in some parts of the study area, suggesting drier and more compact subsurface conditions with lower corrosion potential [17]. Very highly corrosive zones had resistivity values between 23.11 and 70.75 Ω m, whereas highly corrosive zones had resistivity values between 108.7 and 363.3 Ω m. Slightly corrosive zones corresponded to resistivity values between 1234 and 1779 Ω m, moderate corrosive zones ranged from 545 to 871.7 Ω m, and moderate-high corrosive zones ranged from 363.3 to 545 Ω m [15]. These ranges are summarized in Table 7.

4.2. Soil pH distribution

The measured soil pH values in the study area ranged from 6.3 to 7.1, indicating slightly acidic to near-neutral soil conditions. The limited variation in pH values indicates that the chemical properties of the soil are generally consistent across the sampled locations [18, 19]. Particularly in areas with high moisture and salinity levels, the slightly acidic character of some locations may contribute to accelerated electrochemical reactions [19, 31]. A summary of the soil pH distribution is presented in Table 8.

Table 7: Summary of resistivity ranges and corrosion classes.

Resistivity range (Ω m)	Corrosion class
23.11–70.75	Very highly corrosive
108.7–363.3	Highly corrosive
363.3–545	Moderate-high corrosive
545–871.7	Moderate corrosive
1234–1779	Slightly corrosive

Table 8: Summary of soil pH distribution.

Parameter	Value range
Soil pH	6.3–7.1
Dominant condition	Slightly acidic to near-neutral

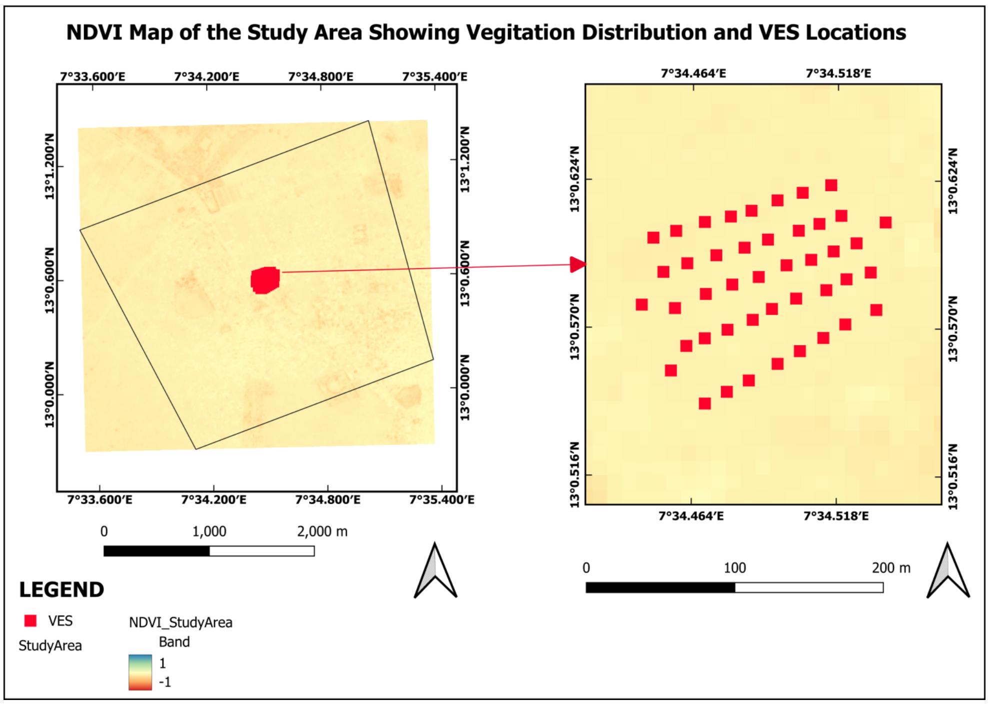

Figure 3: NDVI distribution map.

4.3. *Remote sensing analysis*

The Sentinel-2 spectral indices show spatial variation in environmental conditions across the study area. The NDVI map (Figure 3) shows mostly low vegetation density, with values generally < 0.0 on the index value score. This pattern is consistent with semi-arid environmental conditions, where sparse vegetation cover is associated with increased soil exposure in several locations [22, 23]. The NDWI distribution (Figure 4) shows low moisture zones concentrated primarily within the central portions of the area, with values also generally < 0.0 on the index value score. These zones correspond spatially with low-resistivity zones obtained from the geophysical investigation. The BSI map (Figure 5) indicates low soil exposure in most of the study area, and the salinity index map (Figure 6) shows localized areas with elevated salt concentration, with values of 0.4–0.6 on the index value score [26].

Most vegetation shown on the NDVI map is low, which is consistent with the semi-arid environmental setting. In some locations, limited plant cover is associated with increased soil exposure. The NDWI distribution indicates that low-moisture zones are mostly located within the study area, and these zones spatially correspond to low-resistivity zones identified during the geophysical investigation. The BSI map reveals low bare-soil exposure in most sectors of the study area, while the SI map highlights localized areas with relatively high salt concentrations (Figures 3–6) [26].

4.4. *Corrosion susceptibility index*

In this study, electrical resistivity, soil pH, and remote sensing data from Sentinel-2 were integrated to produce the final corrosion susceptibility index (CSI) map using AHP weight assignment and the WSM. The resulting CSI map is used to classify the study

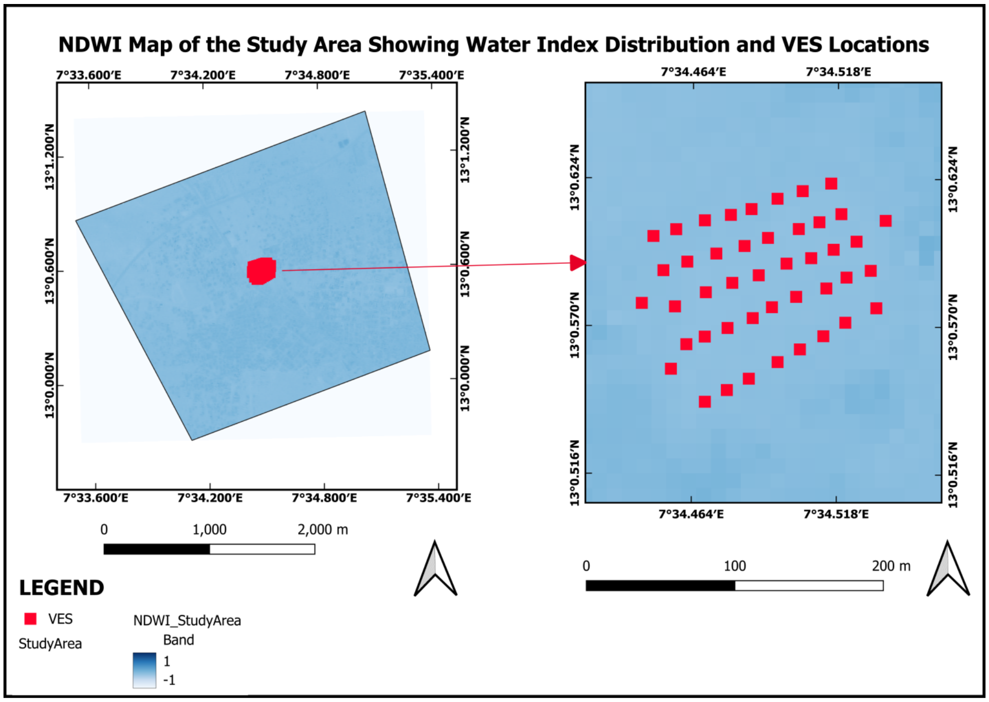

Figure 4: NDWI distribution map.

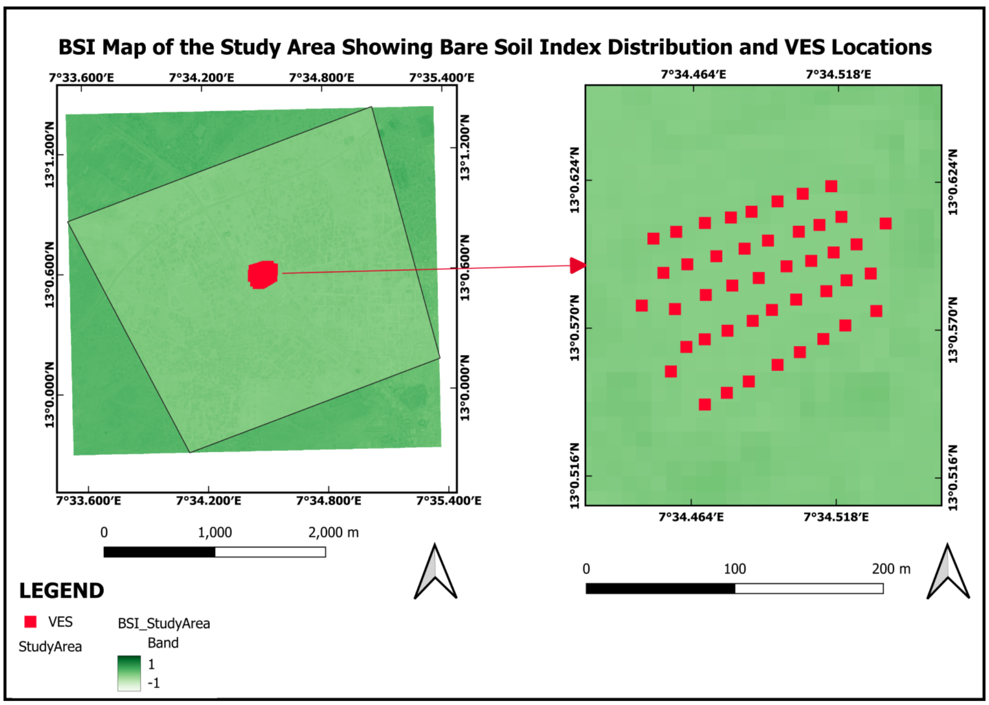

Figure 5: Bare soil index (BSI) map.

area into moderate to high, scale 2-3 corrosion susceptibility levels. The predominant in the research area is moderate corrosion susceptibility. The predominance of moderate susceptibility classes suggests relatively favorable conditions for buried infrastructure; however, site specific investigations are recommended prior to installation.

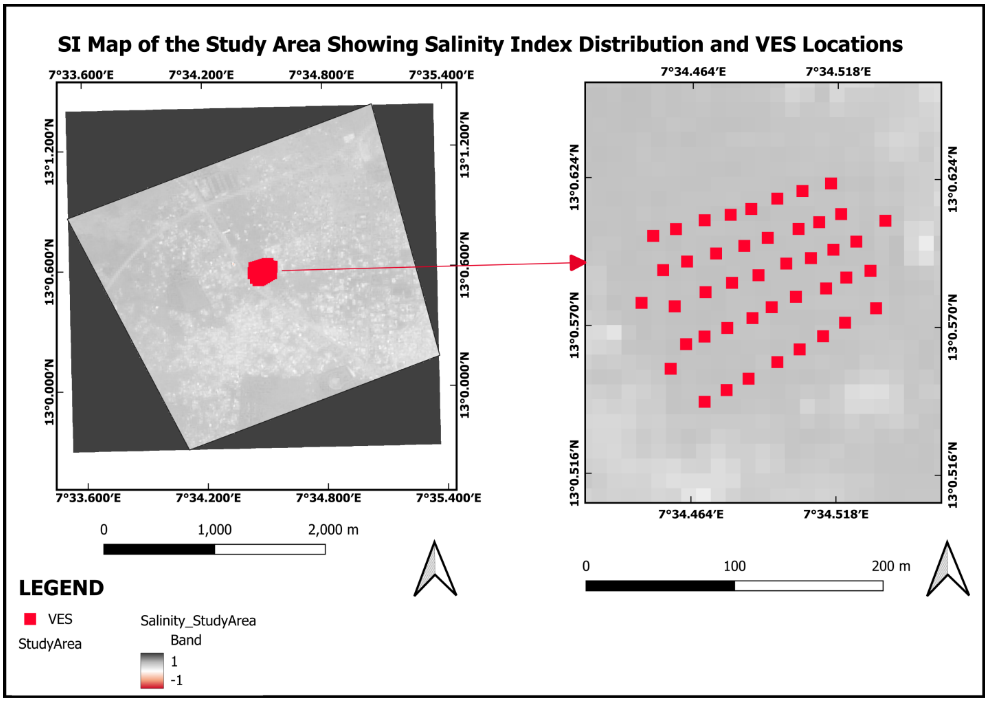

Figure 6: Salinity index (SI) map.

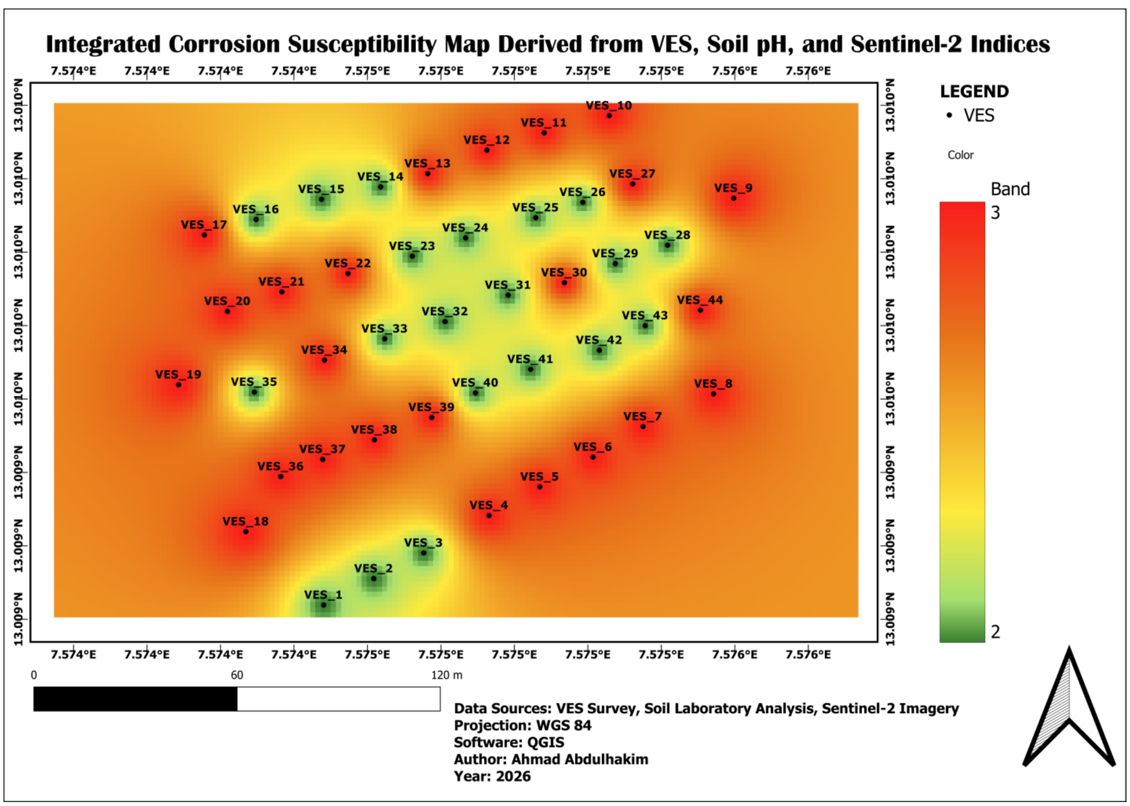

Figure 7: Corrosion susceptibility index (CSI) map.

5. Discussion

The resistivity results presented in Table 7 indicate significant spatial variations in subsurface electrical properties across the study area, suggesting corresponding differences in soil corrosion susceptibility. Soil resistivity is widely recognized as one of the most reliable indicators of soil corrosivity because it reflects the combined effects of moisture content, dissolved salts, soil texture, and ionic concentration [16, 19]. The low resistivity values observed in some locations indicate conditions favorable for electrochemical corrosion processes, whereas higher resistivity zones suggest lower corrosion potential due to reduced conductivity. Similar relationships between low resistivity and increased soil corrosivity have been reported by Akinlabi and Olaiya [30], Irunkwor *et al.* [32], Onyeanwuna *et al.* [33], George [34], and Adeyemo *et al.* [35]. The predominance of moderate corrosion classes within the study area suggests that although severe corrosion conditions are not widespread, localized areas may require corrosion protection measures for buried infrastructure.

The soil pH values presented in Table 8 range from 6.3 to 7.1, indicating slightly acidic to near-neutral soil conditions. Although these values do not represent strongly aggressive chemical environments, mildly acidic soils may still accelerate corrosion reactions when combined with moisture and conductive conditions [19, 31]. The relatively narrow pH range suggests limited spatial variation in soil acidity across the study area. This conclusion is consistent with the findings of Akinlabi and Olaiya [30], who found that, under comparable environmental circumstances, electrical resistivity typically exerts a stronger effect on corrosion susceptibility than pH. The measured pH values show that corrosion susceptibility in the study area is unlikely to be primarily controlled by soil acidity alone.

The NDVI distribution shown in Figure 3 illustrates the spatial variability of vegetation cover within the study area. The whole study area falls below 0.0 on the index value score. The generally low NDVI values are consistent with the semi-arid Sudan Savanna environment and indicate sparse vegetation cover [22, 23]. Increased soil exposure and decreased organic matter formation are frequently linked to areas with limited vegetation. By altering near-surface environmental conditions, these factors may indirectly affect corrosion susceptibility and soil moisture retention. Similar findings have been documented in semi-arid settings where environmental processes and soil physical characteristics are influenced by sparse vegetation cover [5, 6].

The NDWI map shown in Figure 4 reveals spatial variations in surface moisture conditions across the study area, although the whole area shows low values below 0.0 on the index value score. Areas with relatively higher NDWI values indicate greater moisture availability, whereas lower values correspond to comparatively dry surface conditions. Moisture plays an important role in corrosion processes because it facilitates ionic transport and supports electrochemical reactions at the soil–metal interface [19]. Consequently, areas with comparatively higher moisture levels are expected to be more susceptible to corrosion than areas with lower moisture levels. The observed correlation between corrosion susceptibility and moisture conditions is consistent with earlier research that identified soil moisture as a crucial factor affecting corrosion processes [19, 31].

Moisture availability may be a factor in the increased conductivity and corrosion susceptibility shown in some parts of the study area, according to the observed spatial relationship between relatively low-resistivity zones and areas with relatively greater moisture conditions. Similar relationships between electrical resistivity and soil moisture have been documented in previous studies [19].

The spatial distribution of bare-soil conditions is illustrated by the BSI map in Figure 5. Most parts of the study area exhibit relatively low BSI values below 0.0 on the index value score, indicating limited bare-soil exposure. However, localized areas with higher BSI values suggest reduced vegetation cover and increased exposure of the soil surface. Such conditions may influence evaporation rates, soil moisture dynamics, and ultimately corrosion susceptibility. The observed BSI pattern is consistent with the sparse vegetation conditions reflected in the NDVI distribution and supports the environmental characteristics typical of semi-arid regions [8].

The SI map presented in Figure 6 indicates localized zones of elevated salt concentration within the study area. SI values generally range from 0.4 to 0.6 across the study area, indicating moderate to relatively high salinity conditions that may contribute to increased soil conductivity and corrosion susceptibility. Salinity is an important factor in soil corrosivity because dissolved salts increase soil conductivity and enhance electrochemical corrosion processes [27, 31]. Therefore, compared with areas with lower saline conditions, areas with higher SI values may present a higher corrosion risk. Combining salinity data with resistivity and moisture-related characteristics enables a more comprehensive assessment of the environmental variables influencing corrosion susceptibility.

The integrated CSI map shown in Figure 7 demonstrates the combined influence of soil resistivity, soil pH, vegetation cover, moisture conditions, salinity, and soil exposure on corrosion susceptibility. The predominance of low to moderate susceptibility classes suggests that much of the study area may be relatively favorable for buried infrastructure. However, localized zones exhibiting higher susceptibility values indicate areas where corrosion mitigation measures may be required. Similar integrated approaches have been successfully applied in Nigeria for environmental and engineering suitability assessments [32–35]. Compared with single-parameter assessment methods, the GIS-AHP approach used in this study enables informed decision-making for environmental management and infrastructure development by offering a more complete depiction of the spatial diversity of corrosion risk [28].

The use of the AHP framework ensured that the contribution of each parameter to the corrosion susceptibility model reflected its relative importance as established from previous studies and expert judgment. The low CR value of 0.0063 further confirms the reliability of the weighting scheme adopted in the analysis [20].

From an engineering perspective, buried metallic infrastructure, including pipes, underground storage tanks, and foundation materials, may require regular monitoring and suitable corrosion protection measures because of the generally moderate corrosion susceptibility. The identification of limited high-susceptibility zones emphasizes the significance of site-specific investigations before infrastructure development, even though the study area is not characterized by widespread severe corrosion conditions. To maintain long-term infrastructure integrity, corrosion mitigation techniques such as protective coatings, cathodic protection systems, and regular inspection programs may be required in vulnerable areas [16, 36].

5.1. Study limitations

This study assessed soil corrosion susceptibility using electrical resistivity, soil pH, and Sentinel-2-derived environmental indices. However, several limitations should be acknowledged. Soil pH was the only geochemical parameter analyzed, while other important corrosion-related variables, such as chloride concentration, sulfate content, moisture content, organic matter, redox potential, and total dissolved solids, were not evaluated. Furthermore, the corrosion susceptibility model was developed using indirect indicators of corrosion rather than direct corrosion measurements. Field validation using buried metal coupons, pipeline corrosion records, corrosion monitoring systems, or engineering inspection data was not available during the study. Consequently, the generated corrosion susceptibility map should be interpreted as an assessment of potential corrosion risk rather than a direct measurement of actual corrosion rates. Future studies should incorporate additional geochemical parameters and independent validation datasets to improve model reliability.

It should be noted that the spatial extent of the study area where the VES points are located is small. As a result, the variation in color patterns observed in the derived Sentinel-2 index maps may appear limited, as shown in Figures 3–6. Although Sentinel-2 imagery provides relatively high spatial resolution (10–20 m), the indices are calculated at the pixel level, meaning that each pixel represents an average spectral response of the land surface within that area. Consequently, when the study area is small, only a limited number of pixels represent the entire area, which may reduce the visible contrast in color variation across the maps.

6. Conclusion

This study integrated geophysical, geochemical, remote sensing, and GIS techniques to assess soil corrosion susceptibility in Sabon Gida, Katsina State, Northwestern Nigeria. Electrical resistivity data obtained from 44 VES stations revealed significant spatial variations in subsurface conductivity, with resistivity values ranging from 23.11 to 1779 Ω m. Soil pH values ranged from 6.3 to 7.1, indicating slightly acidic to near-neutral soil conditions. Sentinel-2-derived indices further provided information on vegetation cover, moisture distribution, bare-soil conditions, and salinity conditions within the study area.

The integration of resistivity, soil pH, NDVI, NDWI, BSI, and SI using the AHP and WSM produced a CSI map showing predominantly moderate corrosion susceptibility across the study area. The results suggest that the area may be relatively favorable for buried metallic infrastructure; however, site-specific engineering investigations and direct corrosion measurements are recommended before infrastructure installation.

The study demonstrates the usefulness of integrating geophysical, geochemical, and remote sensing datasets within a GIS framework for spatial corrosion susceptibility assessment. Future investigations should incorporate additional geochemical indicators and field validation data to further improve the reliability of corrosion susceptibility models.

Data availability

Data will be made available upon reasonable request from the corresponding author.

Declaration of competing interest

The authors declare that they have no known competing financial interests or personal relationships that could have appeared to influence the work reported in this manuscript.

Funding

The authors received no external funding for this study.

Acknowledgment

The authors sincerely acknowledge the Department of Physics, Federal University Dutsin-Ma, Katsina State, Nigeria, for providing the academic environment and technical support required for this research. The authors are grateful to the field assistants and laboratory technologists who contributed to data acquisition and laboratory analyses. Sentinel-2 satellite imagery used in this study was obtained from the European Space Agency (ESA) through the Copernicus Open Access Hub. The authors also acknowledge the use of IPI2Win, QGIS, and Microsoft Excel for data processing, interpretation, analysis, and visualization.

Abbreviations

AHP, analytical hierarchy process; BSI, bare soil index; CSI, corrosion susceptibility index; GIS, geographic information system; IDW, inverse distance weighting; NDVI, normalized difference vegetation index; NDWI, normalized difference water index; SI, salinity index; VES, vertical electrical sounding; WSM, weighted sum model.

References

[1] M. G. Fontana, *Corrosion engineering*, 3rd ed., McGraw-Hill, New York, USA, 1986. Available online: https://www.google.com.ng/books/edition/Corrosion_Engineering/zcZRAAAAMAAJ?hl=en&gbpv=0&bsq=M.%20G.%20Fontana,%20Corrosion%20Engineering,%203rd%20ed.,%20McGraw-Hill,%20New%20York,%20USA,%201986.

[2] P. R. Roberge, *Corrosion engineering: principles and practice*, McGraw-Hill, New York, USA, 2008. Available online: https://www.accessengineeringlibrary.com/content/book/9780071482431.

[3] W. M. Telford, L. P. Geldart & R. E. Sheriff, *Applied Geophysics*, 2nd ed., Cambridge University Press, Cambridge, UK, 1990. https://doi.org/10.1017/CBO9781139167932.

[4] A. Samouëlian, I. Cousin, A. Tabbagh, A. Bruand & G. Richard, "Electrical resistivity survey in soil science: A review", Soil and Tillage Research **83** (2005) 173. https://doi.org/10.1016/j.still.2004.10.004.

[5] V. L. Mulder, S. de Bruin, M. E. Schaepman & T. R. Mayr, "The use of remote sensing in soil and terrain mapping: a review", Geoderma **162** (2011) 1. https://doi.org/10.1016/j.geoderma.2010.12.018.

[6] F. Castaldi, S. Chabrillat, A. Don & B. van Wesemael, "Soil organic carbon mapping using lucas topsoil database and sentinel-2 data: an approach to reduce soil moisture and crop residue effects", Remote Sensing **11** (2019) 2121. https://doi.org/10.3390/rs11182121.

[7] A. A. Adefolalu, *Climate of Nigeria*, in *Nigeria in maps*, K. M. Barbour, J. S. Oguntoyinbo, J. O. C. Onyemelukwe & J. C. Nwafor (Eds.), Hodder and Stoughton, London, UK, 1983.

[8] K. Abubakar, I. B. Abaje & R. Tukur, "Rainfall and temperature dynamics in the context of climate change in the Sudan Savanna ecological zone of Katsina State, Nigeria", FUDMA Journal of Earth and Environmental Sciences **1** (2024) 82. https://doi.org/10.33003/jees.2024.0102/08.

[9] P. McCurry, "The geology of the Precambrian to Lower Palaeozoic rocks of northern Nigeria", in Geology of Nigeria, C. A. Kogbe (Ed.), Elizabethan Publishing, Lagos, Nigeria, 1976, pp. 15–39. Available online: http://pascal-francis.inist.fr/vibad/index.php?action=getRecordDetail&idt=PASCALGEODEBRGM7720450807.

[10] M. A. Rahaman, "Recent advances in the study of the basement complex of Nigeria", in Precambrian Geology of Nigeria, Geological Survey of Nigeria, Kaduna, Nigeria, 1988, pp. 11–43. Available online: https://cir.nii.ac.jp/crid/1571135650759008768.

[11] A. I. Kankara & N. Shazalli, "Geology and petrography of precambrian rocks of Katsina urban area, Northwestern Nigeria", Zbornik Radova Departmana za Geografiju, Turizam i Hotelijerstvo **49** (2020) 113. https://doi.org/10.5937/zbdght2002113a.

[12] N. G. Obaje, "The basement complex", in Geology and mineral resources of Nigeria, Springer, Berlin, Germany, 2009. https://doi.org/10.1007/978-3-540-92685-6_2.

[13] M. H. Loke, Tutorial: 2-D and 3-D electrical imaging surveys, Geotomo Software, Malaysia, 2004. Available online: https://www.geotomosoft.com/downloads.php.

[14] A. A. Bobachev, IPI2Win v.3.0 and IPI2WinMT: Programs for resistivity and magnetotelluric data interpretation, Moscow State University and Geoscan-M Ltd., Moscow, Russia, 2003. https://x2ipi.voog.com/downloads?utm_source=chatgpt.com.

[15] ASTM G57-20, "Standard test method for field measurement of soil resistivity using the Wenner four-electrode method", ASTM International, West Conshohocken, PA, USA, 2020. https://doi.org/10.1520/G0057-20.

[16] NACE International, Control of external corrosion on underground or submerged metallic piping systems, NACE Standard RP0169, Houston, TX, USA, 2002. https://cir.nii.ac.jp/crid/1570009749298611840

[17] ASTM International, "ASTM G57-06: standard test method for field measurement of soil resistivity using the Wenner four-electrode method", ASTM International, West Conshohocken, PA, USA, 2012. https://doi.org/10.1520/G0057-06R12.

[18] N. C. Brady & R. R. Weil, The nature and properties of soils, 15th ed., Pearson Education, London, UK, 2016. https://www.researchgate.net/publication/301200878_The_Nature_and_Properties_of_Soils_15th_edition

[19] R. W. Revie & H. H. Uhlig, *Corrosion and corrosion control: an introduction to corrosion science and engineering*, 4th ed., John Wiley & Sons, Hoboken, NJ, USA, 2008. https://onlinelibrary.wiley.com/doi/book/10.1002/9780470277270

[20] T. L. Saaty, The analytic hierarchy process, McGraw-Hill, New York, USA, 1980. Available online: https://d1wqtxts1xzle7.cloudfront.net/51627807/saaty-libre.pdf?1486172407=&response-content-disposition=inline\%3B+filename%3DSaaty.pdf&Expires=1784803022&Signature=YAEubaJxZAfFbeyOhYhofPPt8EWmjTsd8dbdBtAabGUu5t~1f3JncBOj1MCOIn5sDPdcGIYC151Nh5pIwY6YDjW04zqJe6hYIkMP9gXxDTFo~~9BYLMyT5Rq~nhKuL2RH2vj68fcNF93Xa8utk2ZPKOptuU9JEAyViwGZIvMs9d72DLAK0I8X0sXs90QGHEp5ijhVRBR8kA7jIB8oCdgVEyG0T5dhPwVZcea~MIVCRXsRnh0DHTTTWstdVpABj-sdlAucRLstnH66~pMbsYvbd8GFlk8dVJJyuURZx0wRi2j9aZuwmgMLq31B0Rlfq6c-vv7IMjPjHkxn9o8RljbaA__&Key-Pair-Id=APKAJLOHF5GGSLRBV4ZA.

[21] J. R. Jensen, *Introductory digital image processing: a remote sensing perspective*, 4th ed., Pearson Education, New York, USA, 2015. Available online: https://www.pearson.com/en-us/subject-catalog/p/Jensen-Introductory-Digital-Image-Processing-A-Remote-Sensing-Perspective-4th-Edition/P200000006907?view=educator&srsltid=AfmBOoqmpMllRoXBXF8m9adLDCisKxvinfUkYdn_J2pvyDeJ1lPrKmb7.

[22] C. J. Tucker, "Red and photographic infrared linear combinations for monitoring vegetation", Remote Sensing of Environment **8** (1979) 127. https://doi.org/10.1016/0034-4257(79)90013-0.

[23] J. W. Rouse, R. H. Haas, J. A. Schell & D. W. Deering, "Monitoring vegetation systems in the Great Plains with ERTS", NASA SP-351 (1974) 309. https://ntrs.nasa.gov/api/citations/19740022614/downloads/19740022614.pdf

[24] S. K. McFeeters, "The use of normalized difference water index (NDWI) in the delineation of open water features", International Journal of Remote Sensing **17** (1996) 1425. https://doi.org/10.1080/01431169608948714.

[25] A. Rikimaru, P. S. Roy & S. Miyatake, "Tropical forest cover density mapping", Tropical Ecology **43** (2002) 39. Available online: https://www.researchgate.net/publication/255718070_Tropical_forest_cover_density_mapping.

[26] Y. Zha, J. Gao & S. Ni, "Use of normalized difference built-up index in automatically mapping urban areas from TM imagery", International Journal of Remote Sensing **24** (2003) 583. https://doi.org/10.1080/01431160304987.

[27] A. A. Hammam & E. S. Mohamed, "Mapping soil salinity in the East Nile Delta using several methodological approaches of salinity assessment", Egyptian Journal of Remote Sensing and Space Sciences **23** (2020) 125. https://doi.org/10.1016/j.ejrs.2018.11.002.

[28] A. Arabameri, B. Pradhan, H. R. Pourghasemi, K. Rezaei & W. Kerle, “A novel approach for assessing watershed susceptibility using weighted overlay and analytical hierarchy process (AHP) methodology”, Environmental Science and Pollution Research **26** (2019) 31981. https://doi.org/10.1007/s11356-019-06355-9.

[29] D. F. Watson & G. M. Philip, “A refinement of inverse distance weighted interpolation”, Geoprocessing **2** (1985) 315. https://cir.nii.ac.jp/crid/1573387450062569472

[30] I. A. Akinlabi & M. L. Olaiya, “Geoelectrical and physicochemical evaluation of soil corrosivity on metallic pipelines: a case study”, Journal of Geography, Environment and Earth Science International **25** (2021) 46. https://doi.org/10.9734/jgeesi/2021/v25i530287.

[31] R. Sadiq, B. Rajani & Y. Kleiner, “Fuzzy-based method to evaluate soil corrosivity for prediction of water main deterioration”, Journal of Infrastructure Systems **10** (2004) 149. https://doi.org/10.1061/(ASCE)1076-0342(2004)10:4(149).

[32] T. C. Irunkwor, C. O. Molua, C. Okobia, D. D. Nmorsi, N. Abanjo, M. Edobor & C. N. Eze, “Geoelectric and geochemical assessment of sub-soil corrosivity and competence for civil infrastructures at Utue-Ogume, Delta State, Nigeria”, Discover Geoscience **3** (2025) 149. https://doi.org/10.1007/s44288-025-00256-w.

[33] U. B. Onyeanwuna, O. C. Akakuru, A. I. Opara, S. O. Onyekuru, S. I. Ibeneme, I. J. Ofoh, G. O. Aigbadon & H. Israel, “Application of geological and geo-electric methods in the assessment of corrosivity, competence, and vulnerability of soils around Southeastern Nigeria”, International Journal of Physical Sciences **19** (2024) 58. https://doi.org/10.5897/IJPS2023.5057.

[34] A. M. George, “Geophysical investigation of subsoil corrosivity within University of Cross River State, Calabar, Southern Nigeria”, Science World Journal **19** (2024) 466. Available online: https://scienceworldjournal.org/article/view/23966.

[35] I. A. Adeyemo, F. O. Korode, O. A. Olaniyan & O. E. Faleye, “Subsurface corrosivity assessment using subsoil resistivity in a typical basement terrain: a case study of the Adebowale Area in Akure, Southwestern Nigeria”, Indonesian Journal of Earth Sciences **4** (2024) A998. https://doi.org/10.52562/injoes.2024.998.

[36] W. von Baeckmann, W. Schwenk & W. Prinz, *Handbook of cathodic corrosion protection*, 3rd ed., Gulf Professional Publishing, Houston, TX, USA, 1997. https://www.amazon.com/Handbook-Cathodic-Corrosion-Protection-Third/dp/0123996511.